Current correlators in QCD (and QED) at zero and finite temperature

Tim Harris

Institute for Theoretical Physics, ETH Zürich

22.06.2026

$$j_\mu = \frac{2}{3}\bar{u}\gamma_\mu u - \frac{1}{3}\bar{d}\gamma_\mu d - \frac{1}{3}\bar{s}\gamma_\mu s + \ldots$$

$$\langle j_\mu(x) j_\nu(0) \rangle$$

$\langle j_\mu(x) j_\nu(0) \rangle$

$T = 0$

SM Precision

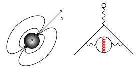

$$\langle j_\mu(x) j_\nu(0) \rangle$$

$T = 0$	$T > 0$
SM Precision	QGP Pheno.

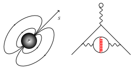

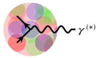

$$\langle j_\mu(x) j_\nu(0) \rangle$$

$T = 0$

$T > 0$

SM Precision

QGP Pheno.

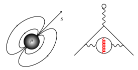

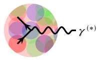

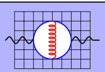

Lattice QCD

Precision QCD and a_μ^{HVP}

- Many results exist for the $I = 1$ window contribution a_μ^{HVP} (left), much fewer are available for the full HVP (right)

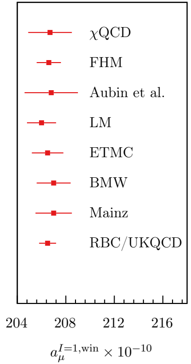

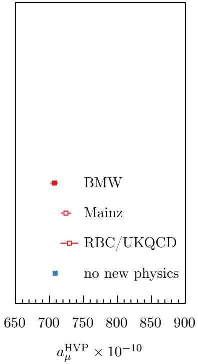

The future focus will be, in particular, on more precise evaluations of ***isospin-breaking effects*** *and the* ***noisy contributions at long distances***[1]***.***

$g-2$ *White Paper 2025*

[1] [2605.00643] TH 2026.

Isospin-breaking corrections

- We typically define QCD through m_π, m_K, f_π, ...
- An ambiguity as $m_{K^\pm} = 494\,\mathrm{MeV} \neq m_{K^0} = 498\,\mathrm{MeV}$ etc. arises at the 1% level!
- To include QED, a perturbative expansion in the small bare parameters

$$e^2/4\pi = 1/137, \qquad a\delta m = a(m_\mathrm{u} - m_\mathrm{d})$$

in the path integral leads to a diagrammatic expansion

$$\langle O \rangle_{\mathrm{QCD+QED}} = \frac{1}{Z} \int DU\, DA\, D\bar\psi\, D\psi\, O\, \underbrace{\left\{1 - \delta m \int \bar\psi\psi - \mathrm{i}e \int j_\mu A_\mu + \ldots\right\}}_{\mathrm{e}^{-S_{\mathrm{int}}}} \mathrm{e}^{-S_{\mathrm{QCD}}} \mathrm{e}^{-S_{\mathrm{Maxwell}}}$$

known as the **RM123 approach**[2], e.g. $O = (\bar{d}\Gamma s)(\bar{s}\Gamma d)$

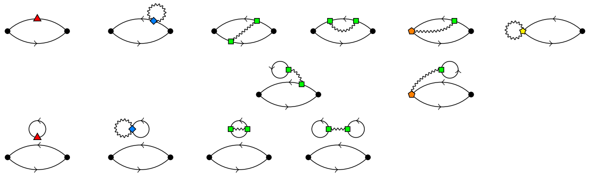

[2] [1303.4896] Divitiis et al. 2013.

Signal-to-noise in the RM123 method

- While the corrections, e.g. w.r.t. the mass, are defined through connected correlators

$$\frac{\partial\langle O\rangle}{\partial a m_f^0} = \langle O a^{-1} \int \bar{\psi}_f \psi_f\rangle - \langle O\rangle\langle a^{-1} \int \bar{\psi}_f \psi_f\rangle$$

the variance of the corresponding estimator does have vacuum contributions[3]

$$\sigma^2_{\delta O} = \langle O^2 \left\{a^{-1} \int \psi_f \psi_f\right\}^2\rangle - \text{ terms with either } \langle O^2\rangle \text{ or } \langle\left\{a^{-1} \int \bar{\psi}_f \psi_f\right\}^2\rangle$$
$$\sim \sigma^2_O \times \frac{L^4}{a^4}$$

which suggests a large statistical uncertainty which is universal (enhanced independent of O)

- An alternative which avoids this issue is **non-perturbative** simulations of the joint QCD+QED distribution

$$\langle O\rangle_{\mathrm{QCD+QED}} = \frac{1}{Z} \int DU\, Dz\, D\bar{\psi}\, D\psi\, O\, \mathrm{e}^{-S_{\mathrm{QCD+QED}}}, \qquad z_\mu(x) = \mathrm{e}^{\mathrm{i} e_0 A_\mu(x)} \in \mathrm{U}(1)$$

→ requires a formulation of QCD+QED in a finite volume

[3] [2301.03995] TH, Gülpers, Portelli, and Richings 2023.

Charged states in a finite volume

- With periodic boundary conditions, admissable gauge transformations $\alpha(x)$ are not completely fixed by a local condition. Consider a gauge transformation

$$\Psi(x) \to \mathrm{e}^{\mathrm{i}2\pi n x_\mu / L}\Psi(x), \qquad A_\mu(x) \to A_\mu(x) + \frac{2\pi n}{L},$$

  which means charged propagators $\langle \Psi(0)\bar{\Psi}(x)\rangle$ vanish after summing on n.

- Such gauge transformations can be excluded by choosing C^* boundary conditions

$$\begin{aligned} A_\mu(x+L) &= A_\mu^{\mathscr{C}}(x) = -A_\mu(x), \\ \Psi(x+L) &= \Psi^{\mathscr{C}}(x) = C^{-1}\bar{\Psi}^\top(x) \end{aligned}$$

  where allowed transformations are $\alpha(x) = \text{anti-periodic} + n\pi$

- This allows a local, gauge-invariant definition of the theory in a finite volume[4]

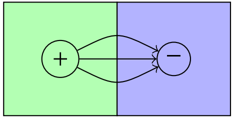

  at the cost of breaking global $\mathrm{U}(1)$ symmetry to $\mathbb{Z}_2$ so that the charge is defined $\bmod 2$

[4] [1509.01636] Lucini, Patella, Ramos, and Tantalo 2016.

Matching QCD+QED in RM123 and non-perturbative formulation

- The same formulation can be used in RM123 and non-perturbative simulation $\rightsquigarrow$ RC* Collaboration[5]
- Tune the bare masses m_f^0 for $f = \mathrm{u}, \mathrm{d}, \mathrm{s}, \mathrm{c}$ to LCP defined by observables at fixed couplings g_0 and $e_0 = e^{\mathrm{phys}}$

$$\left.\begin{aligned} \phi_0 &= 8t_0(M_{K^\pm}^2 - M_{\pi^\pm}^2), \\ \phi_1 &= 8t_0(M_{K^\pm}^2 + M_{\pi^\pm}^2 + M_{K^0}^2), \\ \phi_2 &= 8t_0(M_{K^0}^2 - M_{K^\pm}^2)/\alpha_R, \\ \phi_3 &= \sqrt{8t_0}(M_{D_s^\pm} + M_{D^0} + M_{D^\pm}) \end{aligned}\right\} \quad \text{to take the values} \quad \left\{\begin{aligned} \phi_0 &= 0 & &\neq \phi_0^{\mathrm{phys}}, \\ \phi_1 &= 2.11 & &\approx \phi_1^{\mathrm{phys}}, \\ \phi_2 &= 2.36 & &\approx \phi_2^{\mathrm{phys}}, \\ \phi_3 &= 12.1 & &\approx \phi_3^{\mathrm{phys}} \end{aligned}\right.$$

5[2209.13183] Bushnaq et al. 2022.

Matching QCD+QED in RM123 and non-perturbative formulation

- The same formulation can be used in RM123 and non-perturbative simulation $\rightsquigarrow$ RC* Collaboration[5]
- Tune the bare masses m_f^0 for $f = \mathrm{u}, \mathrm{d}, \mathrm{s}, \mathrm{c}$ to LCP defined by observables at fixed couplings g_0 and $e_0 = e^{\mathrm{phys}}$

$$\left.\begin{aligned} \phi_0 &= 8t_0(M^2_{K^\pm} - M^2_{\pi^\pm}), \\ \phi_1 &= 8t_0(M^2_{K^\pm} + M^2_{\pi^\pm} + M^2_{K^0}), \\ \phi_2 &= 8t_0(M^2_{K^0} - M^2_{K^\pm})/\alpha_R, \\ \phi_3 &= \sqrt{8t_0}(M_{D_s^\pm} + M_{D^0} + M_{D^\pm}) \end{aligned}\right\} \text{ to take the values } \left\{\begin{aligned} \phi_0 &= 0 && \neq \phi_0^{\mathrm{phys}}, \\ \phi_1 &= 2.11 && \approx \phi_1^{\mathrm{phys}}, \\ \phi_2 &= 2.36 && \approx \phi_2^{\mathrm{phys}}, \\ \phi_3 &= 12.1 && \approx \phi_3^{\mathrm{phys}} \end{aligned}\right.$$

This choice corresponds to $M_\pi \approx M_K \approx 400\,\mathrm{MeV}$ $\rightsquigarrow$ `A380a07`

- For RM123 method start with bare parameters $m_\mathrm{u}^0 = m_\mathrm{d}^0$, $e_0 = 0 \Leftrightarrow \phi_2 = 0$ $\rightsquigarrow$ `A400a00`
  and determine the shifts by imposing the above equations to $\mathrm{O}(\alpha)$ and $\mathrm{O}(\delta m_f^0)$

$$\left.\begin{aligned} a\delta m_\mathrm{u}^0 &= -0.00477(13) \\ a\delta m_\mathrm{s}^0 &= -0.00082(17) \\ a\delta m_\mathrm{c}^0 &= -0.0083(28) \end{aligned}\right\} \text{ compatible with } \left\{\begin{aligned} am_\mathrm{u}^0(\phi_2^{\mathrm{phys}}) - am_\mathrm{u}^0(0) &= -0.00476 \\ am_\mathrm{s}^0(\phi_2^{\mathrm{phys}}) - am_\mathrm{s}^0(0) &= -0.000773 \\ am_\mathrm{c}^0(\phi_2^{\mathrm{phys}}) - am_\mathrm{c}^0(0) &= -0.00683 \end{aligned}\right.$$

---

[5] [2209.13183] Bushnaq et al. 2022.

Matching QCD+QED in RM123 and non-perturbative formulation

- The same formulation can be used in RM123 and non-perturbative simulation $\rightsquigarrow$ RC* Collaboration[5]
- Tune the bare masses m_f^0 for $f = \mathrm{u}, \mathrm{d}, \mathrm{s}, \mathrm{c}$ to LCP defined by observables at fixed couplings g_0 and $e_0 = e^{\mathrm{phys}}$

$$\left.\begin{aligned} \phi_0 &= 8t_0(M_{K^\pm}^2 - M_{\pi^\pm}^2), \\ \phi_1 &= 8t_0(M_{K^\pm}^2 + M_{\pi^\pm}^2 + M_{K^0}^2), \\ \phi_2 &= 8t_0(M_{K^0}^2 - M_{K^\pm}^2)/\alpha_R, \\ \phi_3 &= \sqrt{8t_0}(M_{D_s^\pm} + M_{D^0} + M_{D^\pm}) \end{aligned}\right\} \quad \text{to take the values} \quad \left\{\begin{aligned} \phi_0 &= 0 && \neq \phi_0^{\mathrm{phys}}, \\ \phi_1 &= 2.11 && \approx \phi_1^{\mathrm{phys}}, \\ \phi_2 &= 2.36 && \approx \phi_2^{\mathrm{phys}}, \\ \phi_3 &= 12.1 && \approx \phi_3^{\mathrm{phys}} \end{aligned}\right.$$

This choice corresponds to $M_\pi \approx M_K \approx 400\,\mathrm{MeV}$ $\rightsquigarrow$ `A380a07`

- For RM123 method start with bare parameters $m_\mathrm{u}^0 = m_\mathrm{d}^0,\ e_0 = 0 \Leftrightarrow \phi_2 = 0$ $\rightsquigarrow$ `A400a00`
  and determine the shifts by imposing the above equations to $\mathrm{O}(\alpha)$ and $\mathrm{O}(\delta m_f^0)$

$$\left.\begin{aligned} a\delta m_\mathrm{u}^0 &= -0.00477(13) \\ a\delta m_\mathrm{s}^0 &= -0.00082(17) \\ a\delta m_\mathrm{c}^0 &= -0.0083(28) \end{aligned}\right\} \quad \text{compatible with} \quad \left\{\begin{aligned} am_\mathrm{u}^0(\phi_2^{\mathrm{phys}}) - am_\mathrm{u}^0(0) &= -0.00476 \\ am_\mathrm{s}^0(\phi_2^{\mathrm{phys}}) - am_\mathrm{s}^0(0) &= -0.000773 \\ am_\mathrm{c}^0(\phi_2^{\mathrm{phys}}) - am_\mathrm{c}^0(0) &= -0.00683 \end{aligned}\right.$$

$\boxed{\text{Goal: Compare \textit{precision} on predictions via RM123 and non-perturbative approach}}$

[5] [2209.13183] Bushnaq et al. 2022.

Observable: non-singlet vector current correlator

- Although isospin broken, when $\phi_0 = 0$ there is a flavour symmetry between d, s quarks $\Rightarrow N_\mathrm{f} = 1 + 2 + 1$
- Non-singlet U-spin vector current correlator[6]

$$G^\mathrm{U}(x_0) = \int \mathrm{d}^3x \, \langle V_3(x) V_3(0) \rangle, \qquad V_\mu(x) = \tfrac{1}{2}(\bar{s}\gamma_\mu s - \bar{d}\gamma_\mu d)$$

consists only of a valence-connected diagram 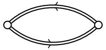

- The corresponding HVP intermediate window contribution with $t_1 = 0.4\,\mathrm{fm}$ and $t_2 = 1\,\mathrm{fm}$

$$a_\mu^\mathrm{U} = \left(\frac{\alpha}{\pi}\right)^2 \int_0^\infty \mathrm{d}x_0 \, G^\mathrm{U}(x_0) K_\mathrm{win}(x_0, t_1, t_2, m_\mu)$$

is 75% of the uds contribution in the $\mathrm{SU}(3)$ flavour limit

[6] [2506.19770] Altherr et al. 2025a.

Results for a_μ^{U} from simulation of QCD and QCD+QED

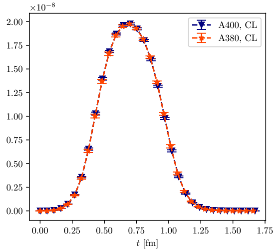

Figure: Simulated integrands for $\phi_2 = 0$ (blue) and $\phi_2 = \phi_2^{\mathrm{phys}}$ (red).

- First compare results for 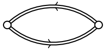 with $\phi_2 = 0$ and $\phi_2 = \phi_2^{\mathrm{phys}}$
- We see only a small effect on the uncertainty from $e_0 = 0$ to $e_0 = e_0^{\mathrm{phys}}$

$$a_\mu^{\mathrm{U}} \times 10^{11} = \begin{cases} 1086(5) & \phi_2 = 0 \\ 1085(7) & \phi_2 \approx \phi_2^{\mathrm{phys}} \end{cases}$$

P. Tavella

Including the corrections in the RM123 method

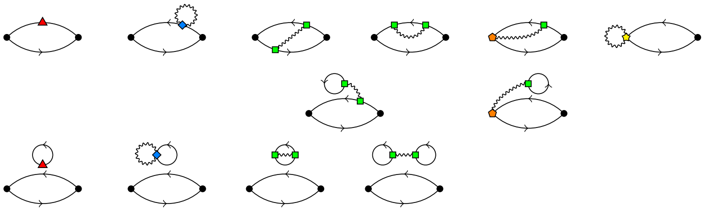


A. Cotellucci, P. Tavella

- For a complete comparison, must take into account the changes to the lattice spacing a and the renormalization factor Z_V

$$a_\mu^\mathrm{U} = \left(\frac{\alpha}{\pi}\right)^2 \int \mathrm{d}x_0\, Z_\mathrm{V} G_\mathrm{bare}^\mathrm{U}(x_0) K_\mathrm{win}(x_0, t_1, t_2, m_\mu), \qquad \delta a_\mu^\mathrm{U} = \delta_G + \delta_Z + \delta_a$$

$$= [12(17) + 1.9(1.7) - 8.4(2.4)] \times 10^{-11}$$

- For the total we arrive at

$$a_\mu^\mathrm{U} \times 10^{11} = \begin{cases} 1092(18) & \text{RM123} \\ 1085(7) & \text{non-perturbative simulation} \end{cases}$$

which shows a huge inflation in the uncertainty due to the RM123 corrections!

C^* boundary conditions: Quo vadis?

- Towards the physical point $\phi_0 \to \phi_0^{\mathrm{phys}}$
  1. Ongoing production project “Tuning QCD+QED simulations with light quarks” 80k node-hours CSCS
  2. EuroHPC proposal submitted → Fall 2026
  3. Finite-volume corrections with C^* boundary conditions in QCD and QCD+QED — P. Tavella (PD), K. Kersic (Ph.D.)
- Simulations with C^* boundary conditions on GPU
  1. PASC1 2022-2025: interface for fields/multi-grid solver with `openQxD/QUDA`[7] — R. Gruber (Ph.D.)
  2. PASC2 2025-2028: offloading Dirac solver/forces in HMC with `openQxD/QUDA` — J. Kuhlmann (PD)
- Compute pure isospin-breaking contribution: a_μ^{38} from the decomposition of the e.m. current $j_\mu = \frac{1}{2} j_\mu^3 + \frac{1}{6} j_\mu^8$

$$G^{38}(x_0) = \int d^3x \, \langle j_k^3(x) j_k^8(0) \rangle, \qquad \lambda^3 = \begin{pmatrix} 1 & 0 & 0 \\ 0 & -1 & 0 \\ 0 & 0 & 0 \end{pmatrix}, \qquad \lambda^8 = \begin{pmatrix} 1 & 0 & 0 \\ 0 & 1 & 0 \\ 0 & 0 & -2 \end{pmatrix}$$

involves the traces $\mathrm{tr}\{S_u \gamma_k S_u \gamma_k\} - \mathrm{tr}\{S_d \gamma_k S_d \gamma_k\} + \mathrm{tr}\{(S_u - S_d)\gamma_k\}\mathrm{tr}\{(S_u - S_d)\gamma_k\}$

Not clear for such observables which approach is more convenient. — A. Altherr (Ph.D.), K. Kersic (Ph.D.)

[7] [2502.02490] Altherr et al. 2025b.

$$\langle j_\mu(x) j_\nu(0) \rangle$$

$T = 0$	$T > 0$
SM Precision	QGP Pheno.
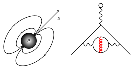	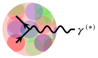

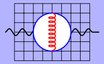

Lattice QCD

Thermal production of photons

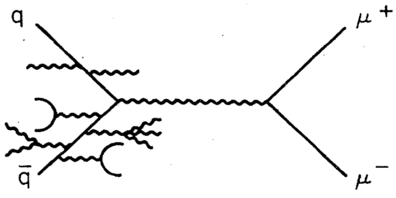

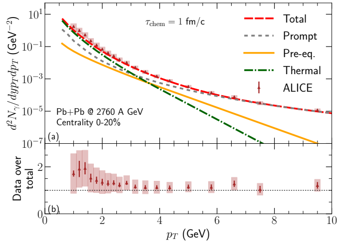

Figure: Leading in α amplitude (left) for virtual photon (dileptons) production and RHIC photon spectrum[8] (right).

- An equilibrated medium of electrically-charged quarks at temperature T emits a thermal spectrum of photons[9]

$$\frac{\mathrm{d}\Gamma_\gamma}{\mathrm{d}\omega} = \frac{\alpha}{\pi}\frac{2\omega}{\mathrm{e}^{\omega/T}-1}\sigma_{\mathrm{T}}(\omega) + \mathrm{O}(\alpha^2)$$

where the spectral function $\sigma_{\mathrm{T}}(\omega)$ is the transverse part of

$$\rho_{\mu\nu}(\omega,\vec{k}) = \int \mathrm{d}t \int \mathrm{d}^3x\, \mathrm{e}^{\mathrm{i}(\omega t - \vec{k}\cdot\vec{x})}\langle[j_\mu(x), j_\nu^\dagger(0)]\rangle \qquad \text{with} \quad \omega^2 = \vec{k}^2$$

[8] [2106.11216] Gale, Paquet, Schenke, and Shen 2022.
[9] McLerran and Toimela 1985.

Dispersion relations at fixed $\vec{k}$

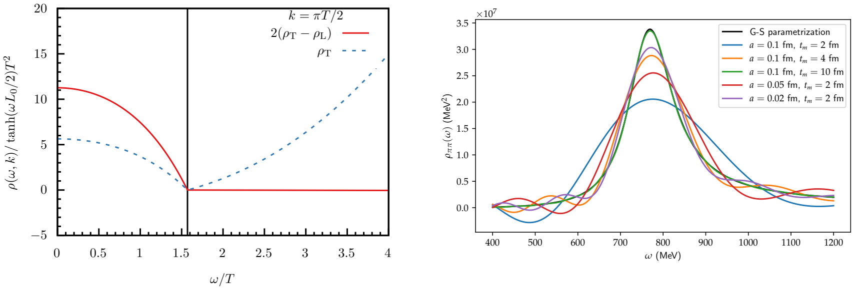

Figure: Leading order spectral densities at fixed $\vec{k}$ (left) and smeared density from the SVD regularization (right).

- The Euclidean time-correlator is related via a dispersion relation to $\rho_{\mu\nu}$ at fixed $\vec{k}$

$$G^{\mathrm{E}}_{\mu\nu}(x_0, \vec{k}) = \int_0^\infty \frac{\mathrm{d}\omega}{2\pi} \frac{\cosh(\omega\{x_0 - L_0/2\})}{\sinh \omega L_0/2} \rho_{\mu\nu}(\omega, \vec{k})$$

  which is sensitive to $Q^2 = -\omega^2 + \vec{k}^2 > 0$ and $Q^2 < 0$ parts of the amplitude.
- With available resolution, impossible to exclude non-lightlike contributions.

I. Staves (M.Sc.)

Dispersion relations at fixed Q

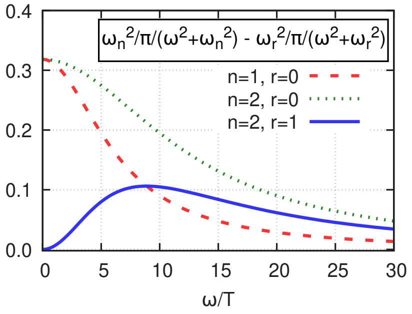

Figure: Kernels for dispersion relation at fixed $Q^2 = 0$ with different $n = 1, 2$.

- Another approach is to notice that a dispersion related at fixed $Q^2 = 0$ exists for the Euclidean correlator[10]

$$H_E(\omega_n) = \int dx_3\, e^{\omega_n x_3} \int dx_0 d\vec{x}_\perp\, e^{-i\omega_n x_0} \langle j_1(x) j_1(0) \rangle = \frac{-\omega_n^2}{\pi} \int_0^\infty \frac{d\omega}{\omega} \frac{\sigma_T(\omega)}{\omega_n^2 + \omega^2}$$

which is the spectrum of $\sigma_T(\omega)/\omega$ “smeared” with a Lorentzian kernel of half-width $\omega_n = 2\pi n T$

[10] [1807.00781] Meyer 2018; [2309.09884] Cè, TH, Krasniqi, Meyer, and Török 2024.

Estimating the ω_1 and ω_2 integrals at $T = 250\,\mathrm{MeV}$

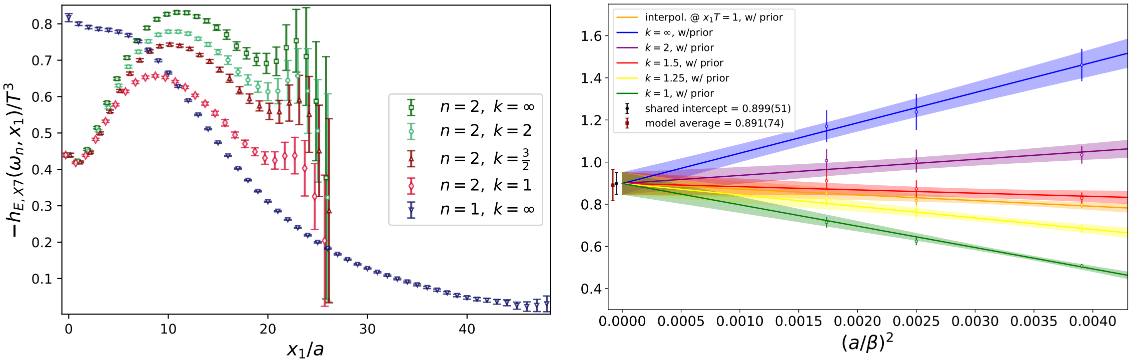

Figure: Integrand for ω_n with $n = 1, 2$ integrals on $L_0/a = 24$ lattice (left) and continuum limit of $n = 2$ integral (right).

- Replacing $\omega_n \to \frac{k}{a}\sin(a\omega_n/k)$ in $\int \mathrm{d}x_3 \mathrm{e}^{\omega_n x_3}$ gives a family of lattice estimators labelled by $k \in \mathbb{R}$[11]
- Continuum limit of $N_\mathrm{f} = 2$ Wilson fermions with $L_0/a = 16, 20, 24$ lattices at $T \approx 250\,\mathrm{MeV}$

[11] [2505.10295] Krasniqi, Cè, TH, Hudspith, and Meyer 2025.

Dealing with the tail contribution

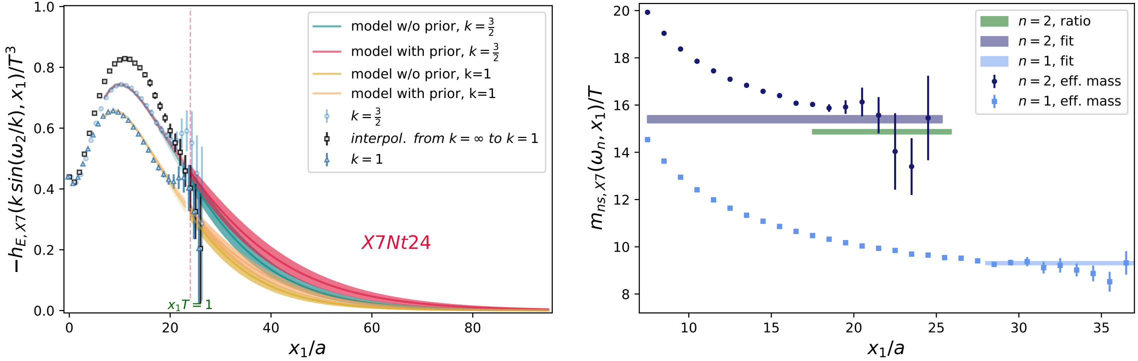

Figure: Integrand ω_2 (left) and non-static effective screening masses (right).

- Integrating the tail we conclude

$$-H_{\mathrm{E}}(\omega_n)/T = \begin{cases} 0.676(7) & n=1 \\ 0.869(74) & n=2 \end{cases}$$

or $-(H_{\mathrm{E}}(\omega_2) - H_{\mathrm{E}}(\omega_1))/T^2 = 0.193(74)$ slightly lower than the LO PT range $0.25 - 0.31$ depending on α_s.

The quark diffusion constant

- The diffusion constant D describes the diffusion of a (heavy) quark at late real times

$$\frac{1}{3}\langle \vec{x}^2(t)\rangle \overset{t\to\infty}{=} 2Dt$$

- The first-order hydrodynamic prediction $\omega \sim 0$ for the transverse density is simply[12]

$$\frac{\sigma_\mathrm{T}(\omega)}{2\chi\omega} = D \quad \to \quad \frac{D}{1+\omega^2/\eta^2}$$

which is expected to be modified in the presence of interactions, form inspired by kinetic theory

- The result $H_\mathrm{E}(\omega_1)$ is compatible with low-ω with parameter D and taking the full LO result for $\omega \gtrsim T$ and a range

$$DT = 0.35 - 0.54$$

which can be compared with other theory predictions

$$DT = \begin{cases} 2.3 & \text{LO PT with } \alpha_\mathrm{s} = 0.25 \\ (2\pi)^{-1} = 0.16 & \text{strong coupling limit of } \mathcal{N} = 4 \text{ SYM} \\ 0.22 - 0.55 & \text{lattice QCD } N_\mathrm{f} = 0 \text{ fixed-}\vec{k} \text{ disp. } \texttt{arXiv:2008.12326} \end{cases}$$

[12] [1003.0699] Hong and Teaney 2010.

Pure gauge theory

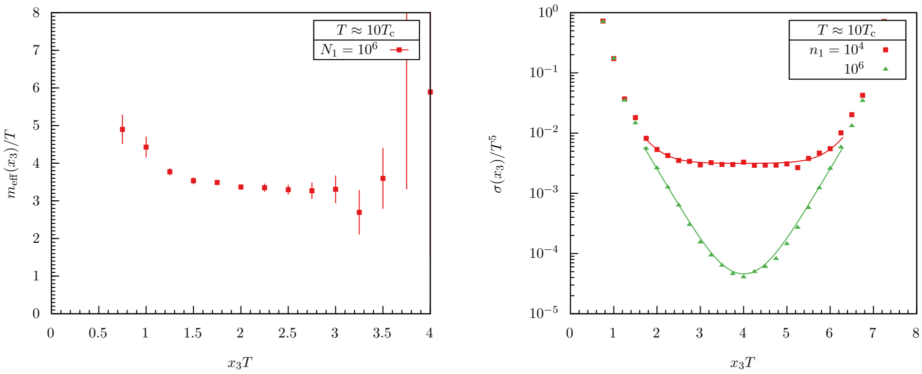

Figure: Multi-level estimation of the pseudoscalar screening length with $T \approx 10T_c$ and its error (right).

- Transport and production rates have analogues in the pure gauge theory: η, ζ, GW spectrum
- Can we control the large-x_3 behaviour in pure gauge theory with the multi-level algorithm?

Summary

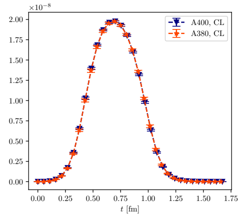

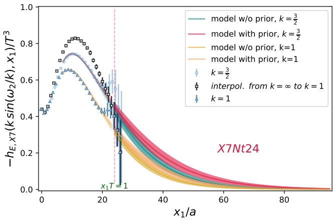

Two frontiers for lattice methods exemplified by $\langle j_\mu(x) j_\nu(0)\rangle$

1. Precision physics and QCD+QED
   - Full simulation with C^* boundary conditions is conceptually and numerically clean
   - Program of $m_\pi \to m_\pi^{\mathrm{phys}}$ with the RC* collaboration
     ⇝ an efficient code on GPU
     ⇝ power-law finite-volume effects
   - What about pure isospin-breaking effects?
2. QCD phenomenology at extreme conditions
   - Fixed-virtuality dispersion relations are an alternative to constrain rates and transport coefficients
     ⇝ Photon rate without contamination
     ⇝ Automatic smearing of the density $\Rightarrow$ well-behaved $L \to \infty$ limit
   - Instead requires control of large-x_3 correlators

References I

[1] TH. “Variance reduction strategies for lattice QCD”. In: *PoS* LATTICE2025 (2026), p. 009. arXiv: 2605.00643 [hep-lat].

[2] G. M. de Divitiis et al. “Leading isospin breaking effects on the lattice”. In: *Phys. Rev. D* 87.11 (2013), p. 114505. arXiv: 1303.4896 [hep-lat].

[3] TH, V. Gülpers, A. Portelli, and J. Richings. “Efficiently unquenching QCD+QED at $\mathrm{O}(\alpha)$”. In: *PoS* LATTICE2022 (2023), p. 013. arXiv: 2301.03995 [hep-lat].

[4] B. Lucini, A. Patella, A. Ramos, and N. Tantalo. “Charged hadrons in local finite-volume QED+QCD with C* boundary conditions”. In: *JHEP* 02 (2016), p. 076. arXiv: 1509.01636 [hep-th].

[5] L. Bushnaq et al. “First results on QCD+QED with C* boundary conditions”. In: (Sept. 2022). arXiv: 2209.13183 [hep-lat].

[6] A. Altherr et al. “Comparing QCD+QED via full simulation versus the RM123 method: U-spin window contribution to a_μ^{HVP}”. In: *JHEP* 10 (2025), p. 158. arXiv: 2506.19770 [hep-lat].

[7] A. Altherr et al. “O(a)-improved QCD+QED Wilson Dirac operator on GPUs”. In: *PoS* LATTICE2024 (2025), p. 280. arXiv: 2502.02490 [hep-lat].

[8] C. Gale, J.-F. Paquet, B. Schenke, and C. Shen. “Multimessenger heavy-ion collision physics”. In: *Phys. Rev. C* 105.1 (2022), p. 014909. arXiv: 2106.11216 [nucl-th].

[9] L. D. McLerran and T. Toimela. “Photon and Dilepton Emission from the Quark - Gluon Plasma: Some General Considerations”. In: *Phys. Rev. D* 31 (1985), p. 545.

References II

[10] H. B. Meyer. “Euclidean correlators at imaginary spatial momentum and their relation to the thermal photon emission rate”. In: *Eur. Phys. J. A* 54.11 (2018), p. 192. arXiv: `1807.00781 [hep-lat]`.

[11] M. Cè, TH, A. Krasniqi, H. B. Meyer, and C. Török. “Probing the photon emissivity of the quark-gluon plasma without an inverse problem in lattice QCD”. In: *Phys. Rev. D* 109.1 (2024), p. 014507. arXiv: `2309.09884 [hep-lat]`.

[12] A. Krasniqi, M. Cè, TH, R. J. Hudspith, and H. B. Meyer. “Probing how bright the quark-gluon plasma glows in lattice QCD”. In: *Phys. Rev. D* 112.7 (2025), p. 074503. arXiv: `2505.10295 [hep-lat]`.

[13] J. Hong and D. Teaney. “Spectral densities for hot QCD plasmas in a leading log approximation”. In: *Phys. Rev. C* 82 (2010), p. 044908. arXiv: `1003.0699 [nucl-th]`.